Thermochimica Acta 486 (2009) 46–51

Contents lists available at ScienceDirect

Thermochimica Acta

journal homepage: www.elsevier.com/locate/tca

Melting point of polymers under high pressure Part II. Influence of gases

Andreas Seeger[a,*], Detlef Freitag[b], Frank Freidel[a], Gerhard Luft[a]

[a] Technische Universität Darmstadt, Ernst Berl-Institut für Technische und Makromolekulare Chemie, Petersenstr. 20, D-64287 Darmstadt, Germany
[b] Friedrich-Alexander-Universität, Erlangen-Nürnberg, Germany

ARTICLE INFO

Article history:
Received 16 September 2008
Received in revised form
23 November 2008
Accepted 16 December 2008
Available online 25 December 2008

Keywords:
Polyethylene
Melting point
Compressed gases
High pressure
DTA

ABSTRACT

The influence of highly compressed gases on the melting of polyethylene was investigated for nitrogen, helium and ethylene. The impact of the particle size of the polymer and the heating rate on the melting point were also analysed. The melting points were determined with a high pressure differential thermal analysis (HPDTA) apparatus. These measurements were compared with independent measurements, done by high pressure differential scanning calorimetry (HPDSC), without gas.

From this experimental data it was possible to calculate the concentration of the gas in the molten polymer phase based on equilibrium thermodynamics. For high density polyethylene (HDPE), a concentration of nitrogen at the polymer melting point of 10.4–35.7 mL(SATP) g(polymer)$^{-1}$, in the pressure interval of 65–315 MPa, was calculated.

1. Introduction

Differential thermal analysis (DTA) is used in our group to investigate the melting of polymers. This technique, invented by Sir Roberts-Austen in 1899 [1], is still one of the most suitable techniques to study thermal phenomena because of the simple design of the measurement cells and the low costs. This is of great advantage when high pressure processes are to be investigated by way of high pressure differential thermal analysis (HPDTA), as we do, for exploring matter surrounded by highly compressed gases.

In various industrial high pressure processes and applications, the knowledge of the melting behavior of polymers with different thermal history and under the influence of different gas atmospheres are of great importance. This is especially true in the case of polymer shaping processes, like injection moulding, film calandration and fabrication of blow films as well, as for polymer particle generation techniques like MIPADIS [2], for safety engineering applications, like the evaluation of the thermal stability of polymer gas tanks and for the prediction of high molecular layers, that can occur on the walls of reactors during the high pressure polymerization of ethylene.

The influence of pressure on the melting of pure components has already been questioned for a long time [3–4]. In case of polymers an increase of pressure leads to an increase of the melting point. This was reported in the literature for high density polyethylene (HDPE) [5–16], ultra high molecular weight polyethylene (UHMWPE)[17], low density polyethylene (LDPE) [10,12] and polypropylene (PP) [18–20]. If the pressure medium is in contact with the sample, then not only the gas pressure but also the type of gas can have an influence on the solid-liquid phase equilibrium, as it was shown for naphtalene and benzene under pressures of nitrogen [21], methane [22], carbon dioxide [23], ethylene [24], xenon [25] and helium [26].

In a preceding work the pressure dependence of the melting point of various polymers, including homo- and copolymers, was investigated under nitrogen atmosphere, by HPDTA. It could be shown, that the melting point always increases with pressure up to 330 MPa. The pressure dependence was found to be in the range of 11–17 K/(100 MPa) [27]. We found that the melting points measured with the HPDTA, under nitrogen atmosphere, were significantly lower than those given in the literature, where the pressure transmitting medium was not in direct contact with the sample. For this reason the polymer was placed in a metal capsule, to ensure that the polymer phase was not contaminated during the experiment. This led us to the ascertainment, that the influence of nitrogen on the melting point, measured with our setup, cannot be neglected above pressures of 10 MPa. Our working hypothesis was, that the gas is partially dissolved in the molten polymer and lowers the melting point of the polymer (colligative effect). To prove this, systematic measurements of the melting point were performed without gas and with nitrogen, helium and ethylene on a standard high density

* Corresponding author. Tel.: +49 6151 16 5446; fax: +49 6151 16 4214.
E-mail addresses: seeger@chemie.tu-darmstadt.de (A. Seeger), luft@bodo.ct.chemie.tu-darmstadt.de (G. Luft).

0040-6031/$ – see front matter © 2008 Elsevier B.V. All rights reserved.
doi:10.1016/j.tca.2008.12.023

polyethylene sample. The impact of the particle size of the polymer and the heating rate were also taken into account.

2. Theoretical background

The binary system under consideration at the melt–freeze equilibrium point, consists of three different phases. Under the premise, that no solid solution of the gas A in the polymer B is developed and that the polymer is not soluble in the gas, we have a system, consisting of a pure gas, that can be supercritical at elevated pressures, a pure solid polymer phase and a liquid polymer phase, acting as a solvent for the most volatile component (gas). It is further assumed, that the molten polymer acting as a solvent for the gas obeys ideal solution laws (see Fig. 1).

The chemical potential (μ) of that part of the component B, that is in the liquid state, is changed by absorption of some gas (component A), lowering the freezing point of the non-volatile component B. The amount of gas, incorporated into the liquid, increases with pressure, thus lowering the freezing point more at higher pressures. Therefore cases can exist, where the melting point can be decreased with an increase of gas pressure, because in that case the chemical potential of the liquid is lowered more by the dissolved gas than increased by pressure [28].

In case of such a binary system, consisting of a gas A, solid B and liquid B with some absorbed A, the chemical potential of the three phases are equal at the equilibrium point (triple point). Therefore an infinitesimal change of the chemical potential can be formulated as follows:

$$d\mu_A^*(g) = d\mu_B(l) = d\mu_B^*(s) \quad (1)$$

If the liquid can be treated as an ideal diluted solution, then Raoult's law is valid and one can write for the chemical potential of the liquid phase:

$$d\mu_B(l) = d\mu_B^*(l) + d(RT\ln x_B) \quad (2)$$

For the liquid to solid phase transition of B it follows:

$$-S_{B,m}(s)dT + V_{B,m}dp = -S_{B,m}(l)dT + V_{B,m}(l)dp + d(RT\ln x_B) \quad (3)$$

With $\Delta S_m = S_{B,m}(l) - S_{B,m}(s) = \Delta H_m/T$, $\Delta V_m = V_{B,m}(l) - V_{B,m}(s)$ and $d\ln x = dx/x$ ($x = x_B$, fraction of the non-volatile component in the liquid phase) we get the following function for the change of the melting point with pressure and composition of the liquid phase [29]:

$$dT = \frac{\Delta V_m T}{\Delta H_m}dp + \frac{RT^2}{x\Delta H_m}dx = \left(\frac{\partial T}{\partial x}\right)_p dx + \left(\frac{\partial T}{\partial p}\right)_x dp \quad (4)$$

With the Henry coefficient $k = dp/dx_A$ it can be formulated:

$$dp = kd(1-x) = -kdx \quad (5)$$

The combination of Eqs. (4) and (5) leads to Eq. (6):

$$dT = -\frac{RT^2}{kx\Delta H_m}dp + \frac{T\Delta V_m}{\Delta H_m}dp \quad (6)$$

With $T = T_f$ and $x = 1$ we get Ipat'ev's equation [30] for the slope of the S–L–G curve at the triple point:

$$\frac{dp}{dT} = \frac{k\Delta H_m}{T_f(k\Delta V_m - RT_f)} \quad (7)$$

Because $k = p/x_A$ Eq. (7) can be transformed to:

$$x_A(p,T) = \frac{p((dp/dT)T_f\Delta V_m^*(T,p) - \Delta H_m^*(T,p))}{T_f^2(dp/dT)R} \quad (8)$$

If the changes in volume $\Delta V_m^*(T,p)$ and enthalpy of fusion $\Delta H_m^*(T,p)$ of the pure component at a certain gas pressure p and fusion temperature T_f are known and we assume that they do not change for the binary system, then the molar fraction x_A of the gas, dissolved in the liquid part of component B, can be calculated.

3. Experimental

3.1. Materials and samples

In the present investigation a commercially available standard high density polyethylene sample was used (HMA 014; Exxon Mobile). If not otherwise noted, this sample was used for the experiments. For the ethene measurements, a low density polyethylene sample was used (LD 151; Exxon Mobile) in order to be closer to the process conditions of the high pressure polymerization. The physical data of these polymers are summarized in Table 1. The given melting points are peak maximum temperatures.

3.2. Sample preparation

For the DTA measurements, either the granulated polymer (as pellets) was used as received from the supplier, or the polymer pellets were ground with a polymer mill, which was cooled by liquid nitrogen, to avoid chain degradation. The milled polymer was directly filled into the DTA cell as a fixed bed, while pellets were attached to the thermocouples according to the following procedure. The pellet was quickly brought into contact with the end of the thermocouple previously heated with the non sooting flame of a Bunsen burner. By this the polymer pellet is partially molten at the contact boundary between the metal mantle of the thermocouple and the polymer pellet; after the polymer solidifies again, the pellet is mounted tight at the top of the thermocouple. This arrangement ensures a direct contact of the polymer to the location of the temperature sensor, which is located under the inconel mantle at the top of the thermocouple.

For the DSC measurements 5 mg of the milled polymer was put into aluminum crucibles, which were then hermetically sealed, to avoid direct contact with the pressure medium.

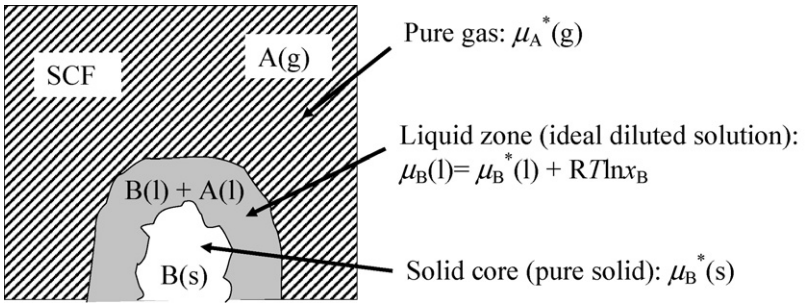

Fig. 1. Three phase S–L–G equilibrium of the binary system of a volatile component A and a non-volatile component B under isochoric conditions (*: pure phase).

Table 1
Polymer data.

Polymer	M_w (10^5 g mol^{-1})	$D = M_w/M_n$ (−)	ρ (g mL^{-1})	$T_{f,0.1\,MPa}$ (K)	MFI (g/(10 min))	$(dT_f/dp)_{N_2}$ (K/(100 MPa))	$\Delta H_{f,0.1\,MPa}$ (J/g)
LDPE							
LD 151	1.73	3.71	0.920	388.9	3	15.8	157.0
HDPE							
HMA 014	2.12	3.03	0.960	403.2	4	16.5	218.8

3.3. Apparatus

The HPDTA cell is designed for pressures up to 350 MPa and temperatures up to 573 K. The sample and the reference cell having an effective volume of 0.7 mL were heated with 2 K/min. The reference cell was left empty. Nitrogen, helium and ethylene were used as pressure medium, which were in direct contact with the sample. A detailed description of the HPDTA can be found elsewhere [27].

The DSC measurements were performed in a power compensated HPDSC, suitable for pressures up to 550 MPa and temperatures up to 300 °C. Details of the construction can be found elsewhere [31]. The calibration was done as usual [32–34].

3.4. Encoding of the experiments

In the experiments the gas, the heating rate and the particle shape was systematically varied. For a better identification of the experiments the following code was used:

A	B	C
Gas:	Heating rates:	Polymer particle conditions:
- He (H)	- 2 K/min (2)	- Powder; milled (M)
- N_2 (N)	- 10 K/min (10)	- Pellet (P)
- Ethene (E)		
- No gas (_)		

For example, an experiment without gas, performed with a milled sample and at a heating rate of 2 K/min, has the code: _2M.

4. Results and discussion

At first high pressure DTA experiments performed under nitrogen atmosphere and high pressure DSC measurements without gas were compared (see Ref. [27]). The slope of the melting curve (dT/dp), measured by HPDTA was lower than the slope that was found by HPDSC, also dT/dp was not constant for the measurements without gas (see Fig. 2). The type of polymer, the sample preparation and the heating rate were kept constant in both series of experiments.

The second step of our analysis was devoted to the impact of other gases dissolved in the liquid polymer, to check whether the magnitude of the gas effect (i.e. a decrease in the melting point value) depends on the amount of gas absorbed in the liquid polymer at the onset of the fusion. In other words, the change in the melting temperature depends on two variables, under the premise that no solid solutions are formed: (i) the solubility of the gas in the molten part of the polymer and (ii) the absorption rate of the gas in question, because one cannot a priori assume that the chosen heating rate is low enough to ensure equilibrium conditions while heating. The amount of gas, that is dissolved in the polymer, should be a function of the strength of the intermolecular forces. In case of ethene, helium and nitrogen, mainly van der Waals interaction forces should have the most impact and should increase with the volume of the particles, as the mobility of the gases in the polymer should decrease with an increase in size of the penetrating gas molecules.

In Fig. 3, the melting point of a LDPE is shown, as a function of pressure under nitrogen and ethene atmosphere. The melting points, measured under ethene atmosphere above pressures of 5 MPa, are much lower than those under nitrogen atmosphere. At ambient pressure the melting point in ethene and nitrogen atmosphere are equal. With increasing pressure the melting point of the polymer, under nitrogen gas, steadily increase, while the melting point with ethene decreases, up to 100 MPa and then increases. So if one would ensure, that the polymer is in the molten state, during an ethene polymerization, one is on the safe side, if one is oriented towards that data, measured under the impact of nitrogen atmosphere.

To decide, whether the particle shape of the polymer has an impact on the melting point or not, milled polymer and polymer

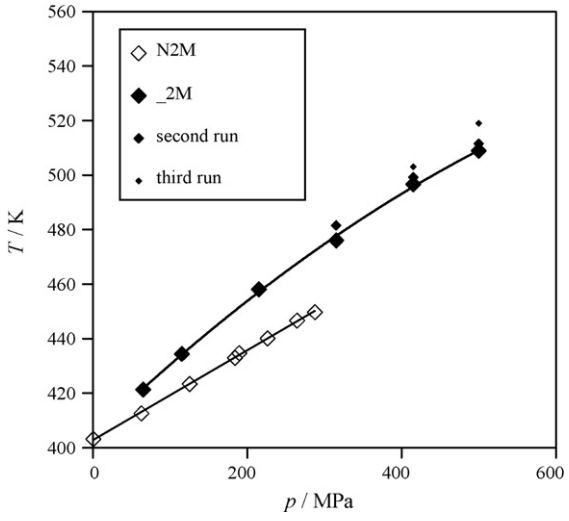

Fig. 2. Comparison of the melting points for a milled HDPE sample, heating rate 2 K/min, measured by HPDSC without gas (full diamonds) and by HPDTA under nitrogen atmosphere (open diamonds).

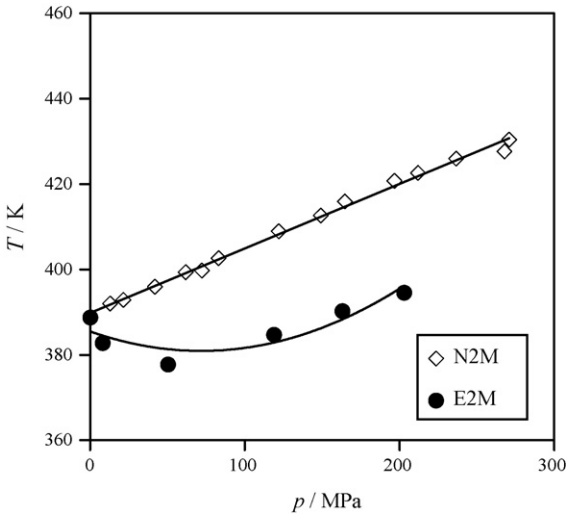

Fig. 3. Comparison of the melting point of an LDPE (LD 151) as a function of pressure for ethylene (curve at bottom) and nitrogen (curve at top).

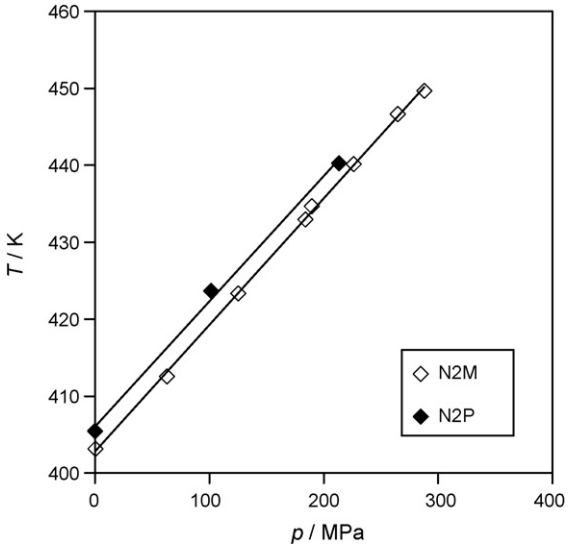

Fig. 4. Influence of the polymer particle size at low heating rate (2 K/min) under nitrogen. N2M: milled polymer, N2P: polymer pellet.

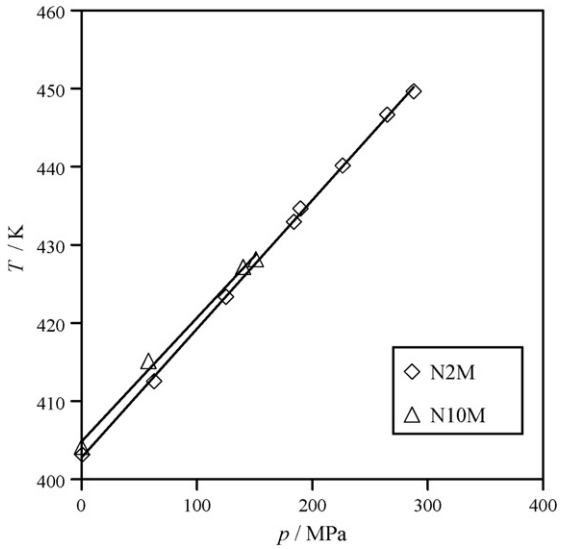

Fig. 6. Influence of the heating rate in case of milled polymer under nitrogen pressure. N2M: 2 K/min, N10M: 10 K/min.

pellets were compared. In Fig. 4 the results of the melting point measurements performed with milled and granulated polymer at a heating rate of 2 K/min are shown. The melting points of the polymer pellets are slightly higher than those, measured for the milled sample. The slopes of both melting curves are similar. This analysis was repeated for a higher heating rate of 10 K/min.

In Fig. 5 the melting points at the higher heating rate of 10 K/min are presented. The melting points determined for the pellets (▲) are up to 4 K higher than those of the milled samples (△) and the slope of the melting curve is not linear for the pellet arrangement. In order to evaluate the influence of the heating rate, the experiments with the same sample shape, but different heating rates, were compared. This is shown in Fig. 6 for the milled HDPE and in Fig. 7 for the granulated sample.

In case of the milled polymer the heating rate has nearly no influence on the melting point, the melting points measured at the higher rates are only two degrees higher, because the measurements at 2 K/min are closer to the melting equilibrium (heating rate: 0 K/min). The influence of the heating rate is much stronger when polymer pellets are used. The reason is, that the rate of the nitrogen adsorption depends on the polymer particle size and the structure of the polymer matrix. The polymer can be saturated much faster with gas, if the polymer surface is large, as in case of small particles.

The experiments show clearly that the melting point is a function of the gas type, the particle size and the heating rate, which is coupled with the time that the gas needs to penetrate into the molten part of the polymer.

In Fig. 8 the melting points measured for helium are shown. In the pressure range of about 70–100 MPa measurements with different particle sizes and heating rates were performed. In that range no significant differences between the melting points, measured for different particle sizes and heating rates were found with the gas helium. Even at a pressure of about 90 MPa the melting points measured at 10 K/min with the polymer pellet (H10P) and the milled polymer at a heating rate of 2 K/min (H2M) did not differ. Whereas with nitrogen, at around 100 MPa (see Fig. 7), a difference in the melting temperatures of about 6 K was observed. This led us to

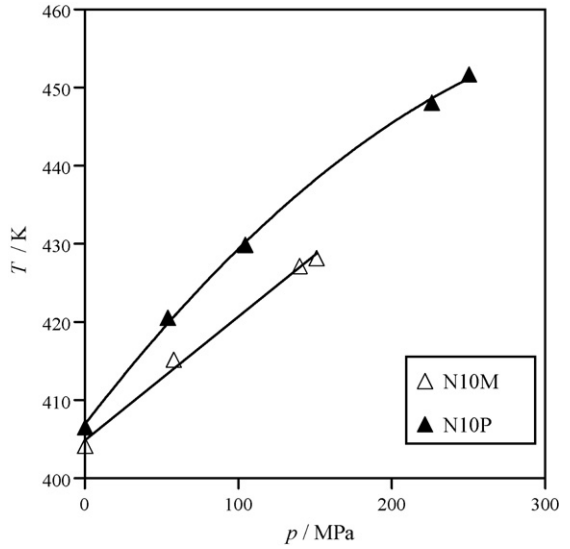

Fig. 5. Influence of the polymer shape at high heating rates (10 K/min) under nitrogen pressure. N10M: milled poylmer, N10P: polymer pellet.

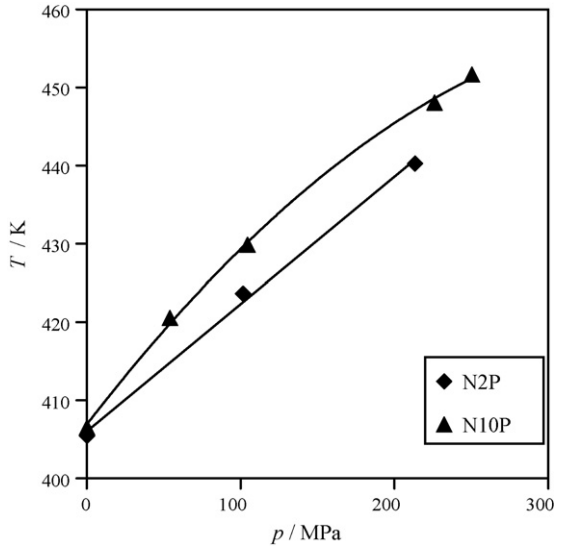

Fig. 7. Influence of the heating rate for polymer pellets under nitrogen pressure. N2P: 2 K/min, N10P: 10 K/min.

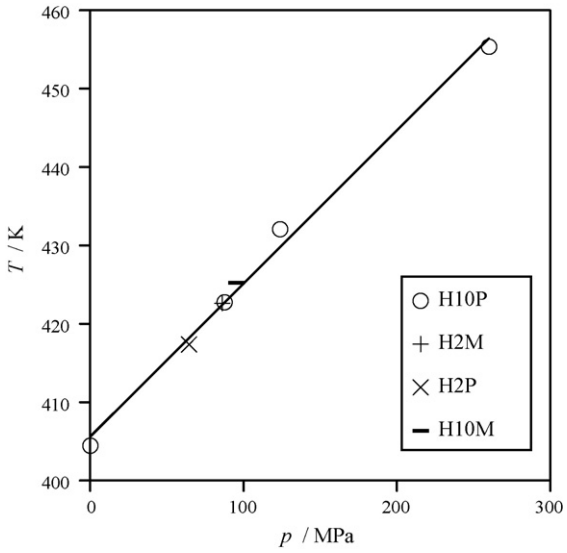

Fig. 8. Melting points of polyethylene under helium atmosphere at different heating rates and particle sizes. H10P: 10 K/min, pellet; H2M: 2 K/min, milled polymer; H2P: 2 K/min, pellet; H10M: 10 K/min, milled polymer.

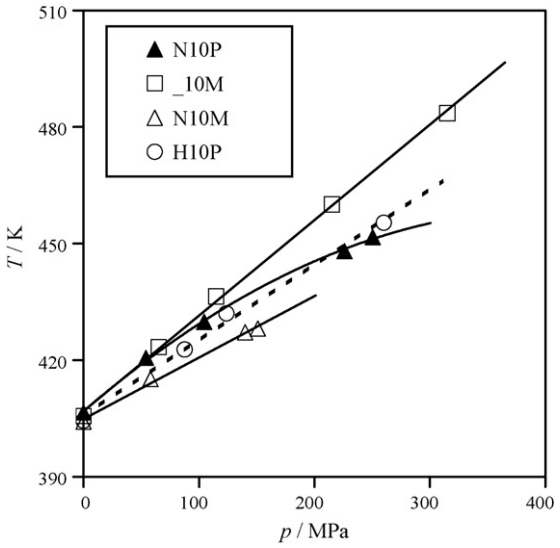

Fig. 9. Comparison of the melting points of HDPE as a function of pressure under nitrogen, helium and without gas at a heating rate of 10 K/min. N10P: nitrogen, pellet; _10M: no gas, milled polymer; N10M: nitrogen, milled polymer; H10P: helium, pellet.

the assumption, that helium is absorbed faster, because the helium atom is smaller than the nitrogen molecule and therefore the penetration rate into the molten polymer matrix should be faster. Data form literature confirm this assumption. For example, it was shown that the diffusion coefficient of helium in polyethylene terephtalate (PET) is significantly higher than that of nitrogen [35].

In Fig. 9 the experiments, at a heating rate of 10 K/min, are summarized. The highest melting points were observed without any gas, while the lowest values were found for the milled polymer under nitrogen atmosphere. The measurements, done with compressed nitrogen, for the pellet arrangement, agree well with the data of experiments without gas, up to 150 MPa. Above this pressure more nitrogen is dissolved in the molten polymer, resulting in a lower melting point. The melting points of the polymer pellets, measured under helium atmosphere, are slightly lower than the melting points, that were determined under nitrogen atmosphere, up to 200 MPa. Above 250 MPa the slope of the melting curve $(dT_f/dp)_{N_2}$ decreases and the fusion points measured in helium are higher.

Based on Eq. (8), the amount of gas, dissolved in the molten polymer was estimated. For the nitrogen measurements, that were performed on the milled polymer, a heating rate of 2 K/min was chosen. We assume here, that this heating rate is low enough to be close at the melting equilibrium. The calculation was done up to 300 MPa. Up to this pressure level, the experiments show clearly, that the melting point is a linear function of pressure for the milled polymer. The data, needed for the pure polymer phase, was extrapolated from the HPDSC experiments done without gas. The experimental results, needed for this calculation and the calculated values, are listed in Table 2.

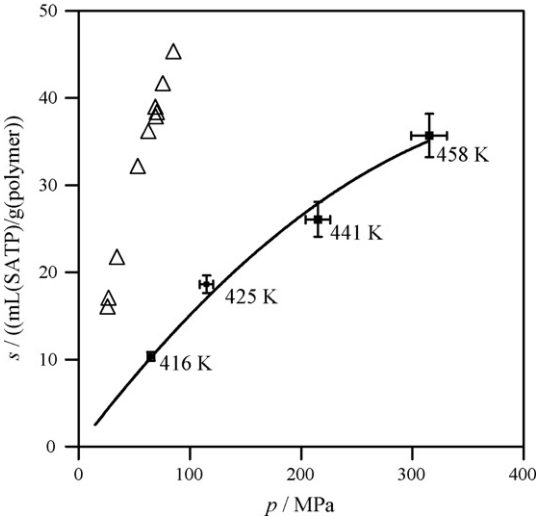

Fig. 10. Amount of nitrogen dissolved in the polymer at the melting point as a function of pressure for HDPE (HMA 014). Δ, Equilibrium solubility of nitrogen in LDPE published by Atkinson at 408 K [36].

In Fig. 10 the calculated solubilities of nitrogen in polyethylene and the corresponding melting temperatures as a function of pressure are shown. At approximately 300 MPa, 35 mL of nitrogen (unit: mL/g, conditions: standard ambient temperature and pressure (SATP)), was absorbed in the liquid polymer phase. For a comparison the equilibrium solubility of nitrogen at 408 K in LDPE, published by Atkinson [36], is also shown. The values are much

Table 2
Solubility of nitrogen in HDPE (HMA 014).

p (MPa)	T^* (K)	$T^\#$ (K)	$(dT/dP)^*$ (10^{-7} K Pa^{-1})	$(dT/dP)^\#$ (10^{-7} K Pa^{-1})	$\Delta H_m{}^*$ (J mol^{-1})	$\Delta V_m{}^*$ (10^{-6} m^3 mol^{-1})	$\Delta S_m{}^*$ (J mol^{-1} K^{-1})	k (Mpa)	s (mL(SATP) g(polymer)$^{-1}$)
65	421.4	416.3	2.43	1.66	4760	2.51	11.3	5616	10.4
115	434.4	424.6	2.43	1.66	5208	2.67	12.0	5581	18.6
215	458.1	441.2	2.43	1.66	4452	2.16	9.72	7514	26.1
315	481.6	457.8	2.43	1.66	4704	2.17	9.77	8125	35.7

* Pure phase.
# Nitrogen charged phase.

higher than our values for HDPE. The reason for these strong deviations is most likely, that the gas absorption has not reached the equilibrium during the DTA experiment. Atkinson has published, that it takes 2 h to reach the absorption equilibrium at a given temperature, but in case of the DTA the time that the gas had to dissolve in the polymer at the melting point temperature was only some minutes.

The results show clearly, that the gas has an influence on the melting process of polyethylene. This is the main reason for the deviations of our data, measured under compressed nitrogen atmosphere, with data from the literature measured with encapsulated polyethylene. A detailed comparison of our data to that given in the literature for pure polyethylene, that was not contacted by compressed gas, can be found elsewhere [27].

The thermal history of the polymer samples often influences the melting point. This can experimentally demonstrated by a HPDTA experiment, which includes subsequent melting and cooling cycles; in this case the melting points detected after the second heating phase are normally higher (Ostwald-Reifung) and this is indeed true for the HDPE sample used in this work (see Fig. 2). In that case not only the thickness of the crystals produce the higher melting point, but above 300 MPa extended chain crystals are formed from the melt [37]. Therefore we used the polymer only from the same batch as received, to ensure comparable thermal history.

The melting behavior is also dependent on the particle size (Gibbs–Thompson effect). Small particles have a lower melting point than larger particles, because the surface to volume ratio is higher for small particles. This effect might be present for the milled polymer, but is of minor importance, because the amount of particles in the submicron range should be low. The helium measurements as well do confirm, that the Gibbs–Thompson effect plays not a major role here and can be neglected, because no significant difference of the melting points between granules and polymer powder could be detected around 100 MPa in case of helium (Fig. 8).

The question, whether solid solutions are formed or not, cannot be answered by our measurements. It is known that gases can be adsorbed at solid surfaces, but the amount of adsorbed gas at solids is lower than the amount of gas that can be absorbed in liquids, hence the solubility of the gas in the liquid should have the strongest influence on the melting point.

5. Conclusion

The melting point of polyethylene is decreased by compressed gas. The melting point depression increases with increasing solubility of the gas in the molten polymer. Even for antisolvents like nitrogen and helium the depression cannot be neglected at high gas pressures. The melting point depression increases with the gas particle size in the range $He < N_2 < C_2H_4$.

Acknowledgements

We thank Prof. G.W.H. Höhne for the high pressure DSC measurements and Exxon Mobile for supplying the polymer samples.

Appendix A. Nomenclature

$(dT_f/dp)_{N_2}$	pressure dependence of the melting point under nitrogen (K/(100 MPa))
D	polydispersity ($D = M_w/M_n$)
ΔH_f	enthalpy of fusion (J/g)
H_m	molar enthalpy (J mol^{-1})
HDPE	high density polyethylene
HPDSC	high pressure differential scanning calorimetry
HPDTA	high pressure differential thermal analysis
k	Henry coefficient (Pa)
LDPE	low density polyethylene
MFI	melt flow index at 2.19 kg (g/(10 min))
M_n	number average molecular weight (g mol^{-1})
M_w	weight average molecular weight (g mol^{-1})
p	pressure (Pa)
R	gas constant ($R = 8.314$ J mol^{-1} K^{-1})
s	solubility (mL(SATP) g(polymer)$^{-1}$)
SATP	standard ambient temperature and pressure
S_m	molar entropy (J mol^{-1} K^{-1})
T	temperature (K)
$T_{f,0.1\,MPa}$	melting point at ambient pressure (K)
V_m	molar volume (m^3 mol^{-1})
x	mole fraction
μ	chemical potential (J mol^{-1})
ρ	density (g/mL)

References

[1] W.C. Roberts-Austen, Fifth report to Alloys Research Commitee, Proc. Inst. Mech. Engrs. 35 (1899) 175.
[2] R. Droegemeier, C. Meister, A. Schottstedt, E. Schweers, U. Bauer, H. Mueller, O. Mientkewitz, patent WO 03/027170, DE 101 45 663.8, 2003.
[3] J.H. Poynting, Proc. Phys. Soc. London 4 (1) (1880) 271.
[4] J.H. Poynting, Phil. Mag. 12 (5) (1881) 32–48.
[5] E. Baer, J.L. Kardos, J. Polym. Sci. A 3 (1965 2827).
[6] R.A. Baltenas, L.A. Igonin, Dokl. Akad. Nauk SSR 163 (1965) 917.
[7] K.H. Hellwege, W. Knappe, P. Lehmann, Kolloid-Z. 183 (1962) 110.
[8] F.E. Karasz, L.D. Jones, J. Phys. Chem. 71 (1967) 2234.
[9] S. Matsuoka, J. Polym. Sci. 57 (1962) 569.
[10] S. Saeki, S. Takei, Y. Ookubo, M. Tsubokawa, T. Yamaguchi, T. Kikegawa, Polymer 39 (18) (1998) 4267.
[11] T. Davidson, B. Wunderlich, J. Polym. Sci. Part A-2 7 (1969) 377.
[12] G.W.H. Höhne, Termochim. Acta 332 (1999) 115.
[13] C. Nakafuku, Polym. J. 27 (9) (1995) 917.
[14] M. Hikosaka, K. Tsukijima, S. Rastogi, A. Keller, Polymer 33 (12) (1992) 2503.
[15] M. Yasuniwa, C. Nakafuku, T. Takemura, Polym. J. 4 (1973) 526.
[16] C. Nakafuku, H. Nakagawa, M. Yasuniwa, S. Tsubakihara, Polymer 32 (4) (1991) 696.
[17] M. Yasuniwa, M. Yamaguchi, A. Nakamura, S. Tsubakihara, Polym. J. 22 (5) (1990) 411.
[18] V.-H. Karl, F. Asmussen, K. Ueberreiter, Makromol. Chem. 178 (1977) 2037.
[19] U. Leute, W. Dollhopf, E. Liska, Colloid Polym. Sci. 256 (1978) 914.
[20] C. Nakafuku, Polymer 22 (1981) 1673.
[21] V.V. de Leeuw, W. Poot, Th.W. de Loos, J. de Swaan Arons, Fluid Phase Equilib. 49 (1989) 75–101.
[22] J.A.M. van Hest, G.A.M. Diepen, The Proceedings of the Symposium on the Physics and Chemistry of High Pressures, London 1962, The Society of the Chemical Industry, 1963, pp. 10–18.
[23] D.M. Lamb, T.M. Barbara, J. Jonas, J. Phys. Chem. 90 (1986) 4210.
[24] C.A. van Gunst, F.E.C. Scheffer, G.A.M. Diepen, J. Phys. Chem. 57 (1953) 578.
[25] M.A. McHugh, J.J. Watkins, B.T. Doyle, V.J. Krukonis, Ind. Eng. Chem. Res. 27 (1988) 1025.
[26] G. Kling, Chem. Ing. Tech. 38 (1966) 1080.
[27] A. Seeger, D. Freitag, F. Freidel, G. Luft, Thermochim Acta 424 (2004) 175.
[28] E. Weidner, J. Knez, Z. Novak, patent WO95/21688, 1995.
[29] J. de Swaan Arons, G.A. Diepen, Recl. Trav. Chim. Pay-bay 83 (1963) 249.
[30] V.V. Ipat'ev, J. Phys. Chem. U.S.S.R 22 (1948) 833.
[31] K. Blankenhorn, G.W.H. Höhne, Thermochim. Acta 187 (1991) 219.
[32] G.W.H. Höhne, H.K. Cammenga, W. Eysel, E. Gmelin, W. Hemminger, Thermochim. Acta 160 (1990) 1.
[33] H.K. Cammenga, W. Eysel, E. Gmelin, W. Hemminger, G.W.H. Höhne, S.M. Sarge, Thermochim. Acta 219 (1993) 333.
[34] S.M. Sarge, E. Gmelin, G.W.H. Höhne, H.K. Cammenga, W. Hemminger, W. Eysel, Thermochim. Acta 247 (1994) 129.
[35] G.E. Serad, B.D. Freeman, M.E. Stewart, A.J. Hill, Polymer 42 (2001) 6929.
[36] E.B. Atkinson, J. Polym. Sci. Polym. Phys. Ed. 15 (1977) 795.
[37] B. Wunderlich, M. Möller, J. Grebowicz, H. Bauer, Adv. Polym. Sci. 87 (1988) 1.